Controlling the Rate of Shuttling Motions in [2]Rotaxanes by Electrostatic Interactions: A Cation as Tunable Brake

Supporting Information

Pradyut Ghosh,[a,c] Guido Federwisch,[a] Michael Kogej,[a] Christoph A. Schalley,*[a] Detlev Haase,[b] Wolfgang Saak,[b] Arne Lützen,*[b] and Ruth M. Gschwind *[a,d]

[a] *Kekulé-Institut für Organische Chemie und Biochemie der Universität, Gerhard-Domagk-Str. 1, D-53121 Bonn, Germany, email: c.schalley@uni-bonn.de*

[b] *Institut für Reine und Angewandte Chemie der Universität, Postfach 2503, D-26111 Oldenburg, Germany, email: arne.luetzen@uni-oldenburg.de*

[c] *Present Address: Central Salt & Marine Chemicals Research Institute, G. B. Marg Bhavnagar 364002, India*

[d] *Present Address: Institut für Organische Chemie der Universität, Universitätsstr. 31, D-93053 Regensburg, Germany; email: ruth.gschwind@chemie.uni-regensburg.de*

1. Synthesis

General synthesis. The synthesis of rotaxanes **1@2 - 1@4** has been carried out utilizing a previously published template effect[1] and is summarized in Schemes S1 and S2. All starting materials were used as obtained from the suppliers without further purification. Solvents were dried according to usual laboratory procedures. ^1H and ^{13}C NMR spectra were recorded in deuterated solvents or solvent mixtures (CD$_2$Cl$_2$, DMF-d_7, CDCl$_3$, CD$_2$Cl$_2$: DMSO-d_6 (1:1), or CD$_2$Cl$_2$: methanol-d_4 (1:1)) on *Bruker* instruments at variable temperatures between 273 K and 353 K at 500.1 (^1H) and 125.8 MHz (^{13}C), at variable temperatures between 193 K and 393 K at 300.1 (^1H), or at 298 K at 400.1 MHz (^1H) or 100.8 MHz (^{13}C), respectively. ^1H NMR chemical shifts are reported on the δ-scale in ppm relative to residual non-deuterated solvent as internal standard. ^{13}C NMR chemical shifts are reported on the δ-scale in ppm relative to the deuterated solvent as internal standard. Signals were assigned on the basis of ^1H, ^{13}C, (and in some cases) ^1H,^{13}C HSQC and ^1H,^{13}C HMBC NMR experiments. FAB (Kratos Concept 1H) and MALDI-TOF (Micromass MALDI-TofSpec-E) mass spectra were recorded using standard matrices (*m*-nitrobenzylic alcohol and 2,5-dihydroxy benzoic acid, respectively). Due to the unavoidable, NMR detectable inclusion of solvent molecules in the solid rotaxanes, only unsatisfying elemental analyses could be obtained. However, the isotope patterns obtained from the MALDI-TOF and ESI-FT-ICR mass spectra are not superimposed

by fragmentations such as hydrogen losses and are in excellent agreement with calculated isotope patterns based on the elemental composition and on natural abundances of isotopes. Exact masses for all rotaxanes were measured with ESI-FT-ICR mass spectrometry and were within 10 ppm mass accuracy.
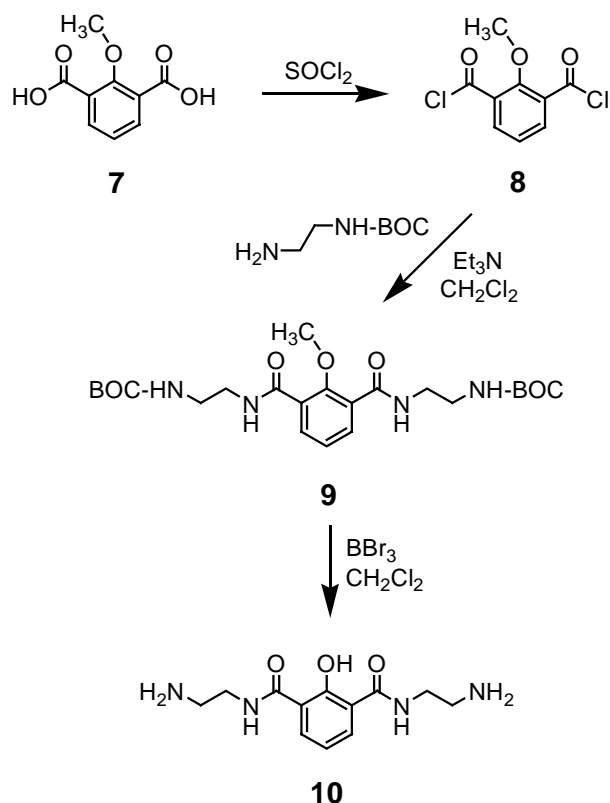
Scheme S1. *Synthesis of axle center piece 10.*

2-Methoxy-isophthalic acid dichloride (8): 3.0 g (15.3 mmol) of 2-Methoxy isophthalic acid **7** were refluxed in a large excess of thionyl chloride in the presence of 2 drops of DMF for 8 hrs. Excess thionyl chloride was removed under reduced pressure. The product was washed with *n*-pentane and dried under Ar. The acid chloride **8** was obtained as a light brown solid in 99% yield. It was used in the next step without further purification.

Boc-protected N,N'-Bis-(2-amino-ethyl)-2-methoxy-isophthalamide (9): 0.7 g (3.0 mmol) of 2-methoxy isophthalic acid dichloride **8** were dissolved in 50 ml dry dichloromethane and added dropwise to a solution of 1.0 g (6.2 mmol) N-Boc-ethylenediamine and 1.2 ml (8.7 mmol) of triethylamine in 50 mL dichloromethane. After complete adition, stirring was continued for 72 h at r.t. The reaction was monitored by TLC (dichloromethane/methanol = 8:1). After completion, the dichloromethane phase was washed with distilled water (3 x 100

ml) dried over anhydrous magnesium sulfate. The solvent was evaporated under reduced pressure and the colorless product was dried. Yield: 86%; m.p. 204 °C ; ^{1}H NMR (400 MHz, CDCl$_3$): δ = 1.38 (s, 18H; Boc-CH$_3$), 3.35 (m, 4H; CH$_2$), 3.55 (m, 4H; CH$_2$), 3.80 (s, 3H; methoxy-CH$_3$), 5.25 (br, 2H; NH), 7.18 (t, 1H; ArH), 7.75 (br, 2H; NH), 7.95 (d, 2H; ArH); ^{13}C NMR (CDCl$_3$): δ = 28.3, 40.3, 46.2, 63.3, 79.4, 124.7, 127.9, 133.9, 156.0, 156.5, 165.8; MS (FAB): m/z = 481.2 [M$^{+•}$].

N,N'-Bis-(2-amino-ethyl)-2-hydroxy-isophthalamide (10): 0.75 g (1.6 mmol) of **9** were dissolved in 50 mL dry dichloromethane and stirred at r.t. under Ar. 2.0 mL (21.2 mmol) boron tribromide was added dropwise over 20 min. After complete addition, stirring was continued overnight at r.t. The reaction was monitored by TLC (dichloromethane/methanol = 15:1). After 20 h, the spot for the reactant almost completely vanished. The reaction was quenched by adding 100 ml methanol then mixture was refluxed for 2 h. The volatiles were evaporated under reduced pressure and this procedure repeated a second time. Then dichloromethane was added to the solid and the mixture was sonicated for 15 min. A pale yellow solid was collected by filtration and dried in vacuum. Yield: 90%; m.p. above 260 °C ; ^{1}H NMR (400 MHz, DMSO-d_6): δ = 3.05 (m, 4H; CH$_2$), 3.62 (m, 4H; CH$_2$), 7.10 (t, 1H; ArH), 7.85-8.10 (m, 6H; 2 ArH and 4 NH$_2$); 8.95 (m, 2H; NH), 14.55 (s, 1H; OH), ^{13}C NMR (DMSO-d_6): δ = 118.5. 118.5, 133.6, 159.9, 168.2; MS (FAB): m/z = 267.1 [MH$^+$]

Triphenyl acetic acid chloride (11): Triphenyl acetic acid chloride **11** was prepared from commercially available triphenyl acetic acid as described for **8** above and used without further purification.

Syntheses of Macrocycles (2, 3, 4): Macrocycles **2**, **3**, and **4** were prepared following well-established literature procedures.[2]

2-Hydroxy-N,N'-bis-[2-(2,2,2-triphenyl-acetylamino)-ethyl]-isophthalamide (1): For comparison with the rotaxane syntheses, 0.08 g (0.3 mmol) axle center piece **10** were suspended in dichloromethane and 96 µL (0.3 mmol) of P1 base was added. **10** dissolved completely within 30 min after base addition in form of its anion. 0.05 ml (0.6 mmol) of triethylamine were added to the mixture and stirred for 5 min followed by 0.18 g (0.6 mmol) of triphenyl acetic acid chloride **11**. The mixture was stirred overnight. The solvent was evaporated and the product was isolated by column chromatography on silica gel using

dichloromethane/ethyl acetate (6:1). Yield: 45%; m.p.203 °C; ^{1}H NMR (400 MHz, CDCl$_3$): δ = 3.45 (m, 8H; CH$_2$), 6.35 (br, 2H; NH), 6.68 (t, 1H; ArH), 6.90-7.25 (m, 30H; CPh$_3$); 7.75 (m, 2H; ArH), 8.25 (br, 2H; NH) 14.55 (s, 1H; OH), ^{13}C NMR (CDCl$_3$): δ = 14.22, 21.05, 39.96, 60.41, 67.91, 118.66, 127.14, 128.06, 130.42, 143.07, 160.40; MS (FAB): m/z = 807.7 [MH]$^{+\bullet}$.

General method for the syntheses of rotaxanes (1@2, 1@3, 1@4): 0.15 mmol of the axle center piece were suspended in 30 mL dry dichloromethane and reacted with 1 eq. of P1 base for 30 min. The center pieces, which were insoluble in dichloromethane, completely dissolved when deprotonated. Then 1 eq. of the corresponding wheel was added to the solution followed by stirring for 2 h. After that time 2 eq. of triethylamine and 2 eq. of triphenyl acetic acid chloride **11** were added. The mixture was stirred overnight. After the solvent was evaporated, the crude product was subjected to column chromatography on silica gel using dichloromethane/ethyl acetate (6:1). Alternatively, the crude product can be partitioned between an organic and a slightly acidic water phase and be subjected to chromatography after drying with MgSO$_4$ and removal of the solvent.

1@2: Yield: 35%; m.p. 219 °C; ^{1}H NMR (500 MHz, DMF-d_7, 333 K): δ = 1.54 (m, 4 H; CH$_2$ (cHex)), 1.64 (m, 8 H; CH$_2$ (cHex)), 2.01 (s, 24 H, CH$_3$), 2.37 (m, 8 H; CH$_2$ (cHex)), 2.99 (m, 4 H; CH$_2$ (-NH(CH$_2$)$_2$NH-)), 3.08 (m, 4 H, CH$_2$ (-NH(CH$_2$)$_2$NH-)), 3.98 (s, 6 H, OCH$_3$), 7.21-7.01 (m, 39 H; CH$_{arom}$ (30 H CPh$_3$, 8 H Me$_2$Ph$_{wheel}$, 1 H HOPh$_{axle}$)), 7.25 (m, 2 H; NH$_{axle}$), 7.62 (m, 4 H, CH$_{arom}$ (MeOPh$_{wheel}$)), 8.07 (d, ^{3}J=7.7 Hz, 2 H, CH$_{arom}$ (CH$_{axle}$ (HOPh$_{axle}$)), 8.52 (s, 4 H, NH$_{wheel}$), 8.53 (m, 2 H, CH$_{arom}$ (MeOPh$_{wheel}$)), 8.71 (m, 2 H, NH$_{axle}$), 15.58 (s, 1 H, OH), ^{13}C NMR (100 MHz, CDCl$_3$, 298 K): δ =18.37, 23.04, 26.34, 45.21, 55.98, 116.91, 118.59, 126.68, 127.48, 128.13, 130.19, 131.30, 135.20, 136.18, 161.15, 165.64; MS (FAB): m/z = 1773.1 [MH$^+$].

1@3: Yield: 33%; m.p. 230 °C; ^{1}H NMR (500 MHz, DMF-d_7, 333 K): δ = 1.45 (s, 9H; tBu), 1.54 (m, 4 H; CH$_2$ (cHex)), 1.64 (m, 8 H; CH$_2$ (cHex)), 2.01 (s, 12 H, CH$_3$), 2.03 (s, 12 H, CH$_3$), 2.37 (m, 8 H; CH$_2$ (cHex)), 3.00 (m, 4 H; CH$_2$ (-NH(CH$_2$)$_2$NH-)), 3.08 (m, 4 H, CH$_2$ (-NH(CH$_2$)$_2$NH-)), 7.20-7.00 (m, 39 H; CH$_{arom}$ (30 H CPh$_3$, 8 H Me$_2$Ph$_{wheel}$, 1 H HOPh$_{axle}$)), 7.25 (m, 2 H; NH$_{axle}$), 7.75 (t, ^{3}J=7.7 Hz, 1 H, CH$_{arom}$ (Ph$_{wheel}$)), 8.08 (d, ^{3}J=7.7 Hz, 2 H, CH$_{arom}$ (CH$_{axle}$ (HOPh$_{axle}$)), 8.12 (dd, ^{3}J=7.7 Hz, ^{4}J=1.1 Hz, CH$_{arom}$ (Ph$_{wheel}$)), 8.17 (d, ^{4}J=1.1 Hz, 2 H, CH$_{arom}$ (tBuPh$_{wheel}$)), 8.48 (s, 2 H, NH$_{wheel}$), 8.58 (m, 2 H, NH$_{wheel}$), 8.72 (m, 2 H,

NH$_{axle}$), 8.77 (m, 1 H, CH$_{arom}$ (*t*BuPh$_{wheel}$)), 8.96 (m, 1 H, CH$_{arom}$ (Ph$_{wheel}$)), 15.61 (s, 1 H, OH), ^{13}C NMR (100 MHz, CDCl$_3$, 298 K): δ = 14.19, 18.35, 18.41, 23.03, 26.33, 31.38, 35.40, 45.18, 60.37, 126.62, 127.43, 128.10, 128.47, 130.16, 131.29, 131.40, 134.55, 134.71, 135.14, 165.72, 166.24; MS (FAB): *m/z* = 1768.2 [MH$^+$].

1@4 Yield: 45%; m.p. above 260°C, ^{1}H NMR (500 MHz, DMF-*d$_7$*, 333 K): δ = 1.46 (s, 9H; *t*Bu), 1.52 (m, 4 H; CH$_2$ (cHex)), 1.63 (m, 8 H; CH$_2$ (cHex)), 1.99 (s, 12 H, CH$_3$), 2.01 (s, 12 H, CH$_3$), 2.29 (m, 4 H; CH$_2$ (cHex)), 2.38 (m, 4 H; CH$_2$ (cHex)), 3.05-2.95 (m, 8 H, CH$_2$ (-NH(CH$_2$)$_2$NH-)), 7.00 (bs, 2 H; NH$_{axle}$), 7.21-7.00 (m, 39 H; CH$_{arom}$ (30 H CPh$_3$, 8 H Me$_2$Ph$_{wheel}$, 1 H HOPh$_{axle}$)), 8.16 (m, 2 H, CH$_{arom}$ (*t*BuPh$_{wheel}$)), 8.17 (d, ^{3}J=8.1 Hz, 2 H, CH$_{arom}$ (CH$_{axle}$ (HOPh$_{axle}$)), 8.40-8.34 (m, 3 H, CH$_{arom}$ (pyridine$_{wheel}$), 8.54 (s, 2 H, NH$_{wheel}$), 8.68 (bs, 2 H, NH$_{axle}$), 8.85 (m, 1 H, CH$_{arom}$ (*t*BuPh$_{wheel}$)), 10.22 (s, 2 H, NH$_{wheel}$), 15.77 (s, 1 H, OH); ^{13}C NMR (100 MHz, CDCl$_3$, 298 K): δ = 18.44, 23.04, 26.36, 31.44, 35.46, 124.81, 127.44, 127.83, 128.27, 130.25, 131.21, 131.54, 134.84, 149.01, 162.04; MS (FAB): *m/z* = 1768.9 [MH$^+$].

2. Characterization of Rotaxanes in the Gas Phase by Mass Spectrometry

Experimental Details. The ESI mass spectra were recorded on a Bruker APEX IV Fourier-transform ion-cyclotron-resonance mass spectrometer equipped with a superconducting 7 Tesla magnet and an Apollo electrospray ion source with off-axis spray needle. The samples were introduced into the source with a syringe pump as a 10 µM methanol solution at a flow rate of ca. 5 µL/min. Parameters − some with a significant effect on signal intensities of the axle-wheel complex − were adjusted as follows: capillary voltage: 4.08 kV; endplate voltage: 3.40 kV; capexit voltage: -95 V; temperature of drying gas: 85°C. The experiments have been carried out with a nebulizer gas pressure of 5 psi and a low drying gas flow. The ions were accumulated in the instruments hexapole for 2 to 4 s. The ions are then introduced into the FT-ICR analyzer cell which was operated at pressures below 10^{-10} mbar and detected by a standard excitation and detection sequence. For each measurement 32 − 256 scans were averaged to improve the signal-to-noise ratio.

For MS/MS experiments, the whole isotope patterns of the ion of interest were isolated by applying correlated sweeps, followed by correlated shots to remove the higher isotopes. After isolation, argon was introduced into the ICR cell as the collision gas through a pulsed valve at a pressure of ca. 10^{-8} mbar. The ions were accelerated by a standard excitation protocol and detected after a 2 s pumping delay. A sequence of several different spectra was recorded at

different excitation pulse attenuations in order to get at least a rough and qualitative idea of the effects of different collision energies on the fragmentation patterns.

3. Characterization of Rotaxanes 1@2 and 1⁻@2 in Solution by ^{1}H NMR Spectroscopy

Experimental Details. NMR data were collected at 233 K on a Bruker DMX spectrometer operating at a ^{1}H-resonance frequency of 500 MHz using a 5-mm triple-resonance TBI(^{1}H/^{13}C/X) probe with pulsed field gradients in z-direction. From variable temperature measurements optimal linewidths of the proton signals were obtained at 233 K. Therefore, this temperature was chosen for the characterization of the structures and the dynamic behaviors of the two rotaxanes. The assignments of the ^{1}H and the ^{13}C chemical shifts were achieved by a combination of ^{1}H,^{1}H COSY, ^{1}H,^{1}H NOESY, ^{1}H,^{1}H ROESY, ^{1}H,^{13}C HSQC and ^{1}H,^{13}C HMBC spectra for **1@2** (ca. 0.01 M) in a mixture of CD_2Cl_2 and DMSO-d_6 and for **1⁻@2** (ca. 0.04 M) in CD_2Cl_2 +10% DMSO-d_6 at 233 K (see Table 4). No significant chemical shift differences were observed by changing the solvent. For the structural characterization of **1@2** and **1⁻@2,** several ^{1}H,^{1}H NOESY spectra with different mixing times (50, 100 and 500 ms) and a ^{1}H,^{1}H ROESY spectrum of **1@2** with a mixing time of 300 ms were recorded. All significant NOE cross peaks being characteristic for the position of the wheel relative to the axle found in the NOESY spectra with 500 ms mixing time were also observed in the NOESY and ROESY spectra with shorter mixing times. For the determination of the rate constants of the shuttling movement the diagonal and the cross signals of the ethylene protons of the axle in the NOESY spectra with a mixing time of 500 ms were used (see below). The rate constants k were calculated with the following equation.[3]

$$k = \left[t_{mix}(I_{dia} / I_{cross} + 1) \right]^{-1}$$

(I_{dia}= Intensity of the diagonal signal; I_{cross}= Intensity of the cross signal; t_{mix}= mixing time)

Table S1. ^{1}H and ^{13}C chemical shifts of deprotonated $\mathbf{1^-@2}$ in CD_2Cl_2 + 10 % DMSO-d_6 and of neutral $\mathbf{1@2}$ in a mixture of CD_2Cl_2 and DMSO-d_6 at 233 K.[a]

Wheel	$\mathbf{1^-@2}$	$\mathbf{1^-@2}$	$\mathbf{1@2}$
W^1_a	3.89	55.0	3.92
W^2_a	-	159.4	-
W^3_a	7.57	115.0	7.62
W^4_a	-	114.8	-
W^5_a	8.71	119.0	8.50
W^1_b	3.93	56.0	3.92
W^2_b	-	159.7	-
W^3_b	7.50	115.0	7.52
W^4_b	-	114.8	-
W^5_b	8.17	118.3	8.16
W^7_a (NH)	9.41	-	8.74
W^7_b (NH)	7.96	-	7.74
W^9	-	132.0	-
$W^{10\ b)}$	1.63, 1.82, 1.82, 2.12	-	1.62, 1.80, 1.80, 2.12
$W^{11\ b)}$	7.15, 6.63	125.9, 127.3	-
Axle			
A^a_c	6.55	126.2	-
A^a_f	7.12	125.7	-
A^b_c	6.98	126.2	-
A^b_f	7.13	126.9	-
A^c_c	6.54	129.2	6.55
A^c_f	7.17	129.6	7.20
A^d_c	-	66.3	-
A^d_f	-	66.7	-
A^f_c	-	175.2	-
A^f_f	-	172.3	-
A^g_c (NH)	5.75	-	5.21
A^g_f (NH)	7.20	-	6.85
A^h_c	2.13	37.5	2.12
A^h_f	3.33	40.7	3.59
A^i_c	2.07	35.4	2.10
A^i_f	3.40	37.0	3.44
A^j_c (NH)	12.17	-	8.54
A^j_f (NH)	11.96	-	8.69
A^k_c	-	170.2	-
A^k_f	-	168.9	-
A^l_c	-	119.5	-
A^l_f	-	118.3	-
A^m	-	171.6	-
A^n_c	7.76	133.0	8.03
A^n_f	7.83	133.7	7.44
A^o	6.21	108.2	6.77
A^p (OH)	-	-	15.59
P1-base			
NH_{P1}	5.49	-	-
NMe_{P1}	2.61	37.2	-
tBu_{P1}	1.18	31.2	-

[a] *not assigned chemical shifts were omitted. For the nomenclature, see Scheme S3.*

[b] *the individual methyl groups and the meta positions of the aromatic rings in the wheel could not be differentiated.*

Table S2. X-ray crystal structure data for **1@2**.

Identification code	$C_{114}H_{114}N_8O_{11}$ * $6(OHCH_3)$
Empirical formula	$C_{120}H_{138}N_8O_{17}$
Formula weight	1964.38
Temperature	193(2) K
Wavelength	0.71073 Å
Crystal system	Triclinic
Space group	P-1
Unit cell dimensions	a = 14.9686(5) Å $\quad\quad$ α= 102.373(5)°.
	b = 17.0315(8) Å $\quad\quad$ β= 91.482(5)°.
	c = 24.6488(11) Å $\quad\quad$ γ = 107.245(5)°.
Volume	5835.1(4) Å^3
Z	2
Density (calculated)	1.118 Mg/m^3
Absorption coefficient	0.075 mm^{-1}
F(000)	2100
Crystal size	0.50 x 0.23 x 0.21 mm^3
Theta range for data collection	2.11 to 26.01°.
Index ranges	-16<=h<=16, -20<=k<=20, -30<=l<=30
Reflections collected	72811
Independent reflections	21332 [R(int) = 0.0871]
Observed reflections	9109 [I>2sigma(I)]
Completeness to theta = 26.01°	92.9 %
Absorption correction	None
Max. and min. transmission	0.9845 and 0.9637
Refinement method	Full-matrix least –squares on F^2 with SHELX-97[4]
Data / restraints / parameters	21332 / 10 / 1086
Goodness-of-fit on F^2	1.048
Final R indices [I>2sigma(I)]	R1 = 0.1215, wR2 = 0.3191
R indices (all data)	R1 = 0.2041, wR2 = 0.3678
Largest diff. peak and hole	1.175 and -1.023 e.Å^{-3}

4. Characterization in the Solid State by X-ray Crystallography

Experimental details. Single crystals suitable for X-ray crystallography were grown by slowly evaporating CH_2Cl_2 from a saturated solution of rotaxane **1@2** in CH_2Cl_2/MeOH (1:1). The most important crystal structure data are given in Table S2. All non-hydrogen atoms were anisotropically refined and the H atoms were inserted in the calculated positions. The poor R-values are mainly due to strong disorder effects of the solvent molecules found in

the structure. It should be mentioned, that there are three groups of the rotaxane structure that also show some disorder effects. These are one phenyl ring in one of the triphenylene stoppers of the axle, for which a 50:50 distribution between two positions was observed, one of the spirolinked cyclohexylrings of the wheel (70:30 distribution), and one isophthalamide unit of the wheel (50:50). Thus, several very short hydrogen-hydrogen contacts can be found in the structure belonging to one or the other position of the disordered atoms. These disorder effects, however, do not have any influence on the proof of the rotaxane structure itself or the observation of the wheel's position along the axle. The detailed description of the crystal structure can be found. A description of the crystal structure can be found in the CIF file accompanying this paper. CCDC- 230812 contains the supplementary crystallographic data for this paper. These data can be obtained free of charge via www.ccdc.cam.ac.uk/conts/retrieving.html (or from the Cambridge Crystallographic Data Centre, 12, Union Road, Cambridge CB21EZ, UK; fax: (+44) 1223-336-033; or deposit@ccdc.cam.ac.uk).

6. Force Field and AM1 Calculations

Details of Calculations. AM1 calculations[5] were performed[6] with the MOPAC algorithm implemented in the Cache 5.0 program package.[7] The structures chosen for these calculations were generated with 3000 step Monte Carlo conformational searches of favorable conformations with the Amber* force field[8] implemented in MacroModel 8.[9] The lowest energy conformers out of 3000 structures were determined by placing closure bonds in the macrocycles (one of the amide bonds) and the attached cyclohexyl side chains. While the aromatic rings and the amides were constrained to planarity, all single bonds (with the exception of the methyl groups) were selected to allow rotations into other conformations. For each minimization, the number of iterations was set to 10.000 in order to generate fully converged structures. The energy range for structures to store in the output file was set to 50 kJ/mol above the lowest energy conformer. The best conformations and several less favorable alternatives were then reoptimized at the AM1 level of theory. Generally, the force-field calculations and the AM1 results are in good agreement with each other.

Additional theoretical results not discussed in the main text. In the following section, additional theoretical data is discussed in support of the calculations presented in the main text. Since the rotaxanes are quite large systems for a concise theoretical treatment, we made use of a stepwise approach. First, the axle centerpieces and the components of the rotaxanes

Table S3. Heats of formation ΔH_f (kJ/mol) for the rotaxanes and their components and some analogous guest molecules as calculated at the AM1 level of theory and binding enthalpies ΔH_{assoc} (kJ/mol) of non-covalent complexes under study.

compound	conformation	ΔH_f (kJ/mol)	ΔH_{assoc} (kJ/mol)
		single components	
10		-405.5	
10⁻		-601.9	
5'	all-in [a]	-146.7	
5'	3-in-1-out [a]	-145.5	
5'	2-in-2-out [a]	-144.7	
6'		-101.6	
1		109.1	
1⁻		-107.0	
15		-326.4	
16		-93.2	
16⁻		-171.8	
17⁻		-382.9	
18		-190.2	
19		-600.7	
		axle center piece - wheel complexes	
10⁻•5	non-threaded	-865.6	-117.0
	threaded	-861.5	-112.9
10⁻•6'	non-threaded	-807.6	-104.1
	threaded (a) [b]	-806.3	-102.8
	threaded (b) [b]	-803.4	-99.9
		wheel - guest complexes	
15•5		-534.2	-61.1
16•5		-254.1	-14.2
16⁻•5		-456.9	-138.4
17⁻•5		-668.0	-138.3
18•5		-392.9	-56.0
19•5		-787.9	-40.5
		rotaxanes with protonated axle center piece	
1@5	type I [c]	-106.6	-69.0
	type II [c]	-92.4	-54.8
	type III [c]	-86.9	-49.3
1@5	type Ia [b,c]	-51.0	-58.5
	type Ib [b,c]	-56.8	-64.3
	type IIa [b,c]	-39.3	-46.8
	type IIb [b,c]	-38.9	-46.4
	type IIIa [b,c]	-39.7	-47.2
	type IIIb [b,c]	-34.7	-42.2
		rotaxanes with deprotonated axle center piece	
1⁻@5	type I [c]	-350.3	-96.6
	type II [c]	-345.5	-91.8
	type III [b]	-345.3	-91.6
1⁻@6	type Ia [b,c]	-295.5	-86.9
	type Ib [b,c]	-294.3	-85.7
	type IIa [b,c]	-295.1	-86.5
	type IIb [b,c]	-293.0	-84.4
	type IIIa [b,c]	-290.1	-81.5
	type IIIb [b,c]	-282.2	-73.6
		deprotonated rotaxanes with P1 cation	
1⁻@5•P1⁺	type I [c]	-267.9	
	type III [c]	-237.4	

[a] *Assignment of conformations of the wheel: "in" refers to the NH part of the amide group pointing into the cavity of the wheel, "out" to the amide proton pointing away from the cavity.* [b] *Since the pyridine wheel is not symmetric, two analogous conformations of each type are possible. "a" and "b" denote conformations with the phenolate oxygen pointing away from or towards the pyridine nitrogen atom of the wheel, respectively.* [c] *For the assignment of type I - III, see Figure 9 (main text).*
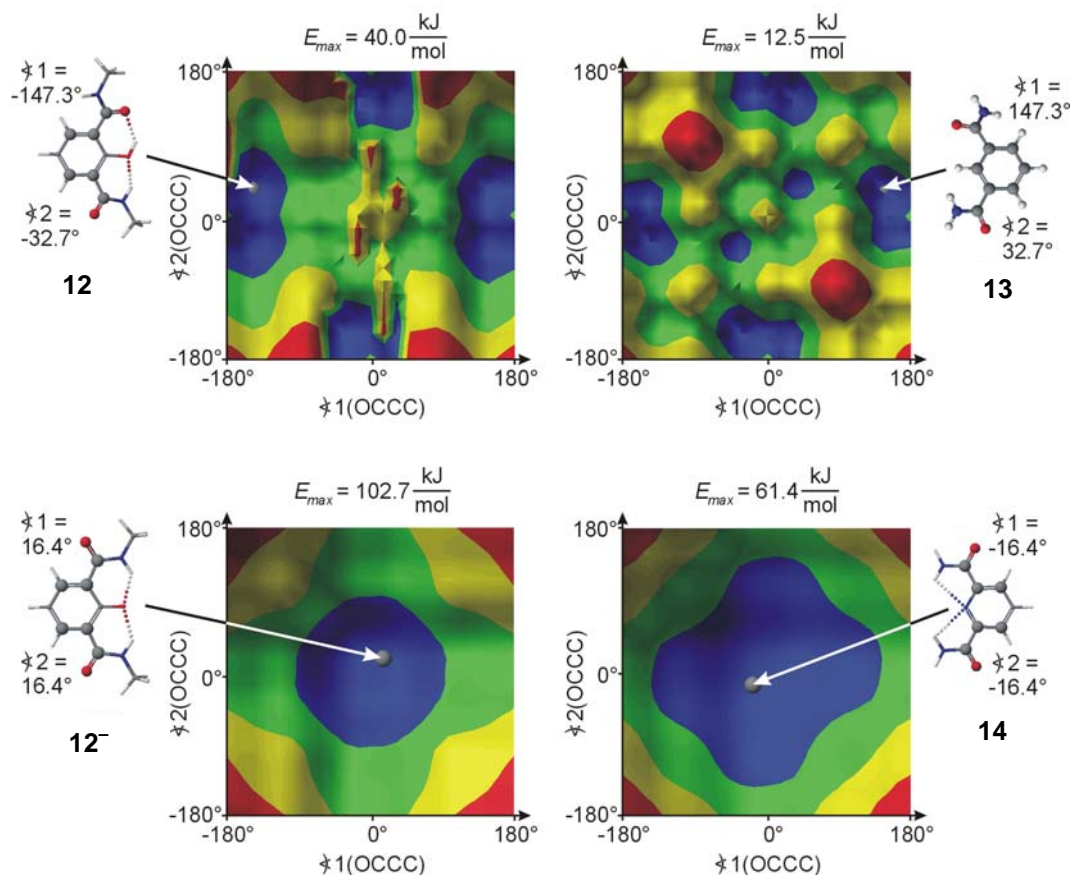
Figure S1. *Potential energy contour maps for rotations about the dihedral OCCC angles defined by the atoms depicted as spheres for the four isophthalic acid dicarboxamide derivatives **12** - **14** shown. The structures shown represent the global minima (indicated in the contour map by gray spheres). Dotted lines in the structural formulae represent hydrogen bonds. Energies are indicated by colors and range from blue (low energies) to red (high energies; E_{max} values indicate highest energies above the global minimum of each surface).*

were examined separately (Table S3). For the identification of favorable conformations, the various isophthalic acid dicarboxamide derivatives incorporated in the axle and the wheels are of importance, because intramolecular hydrogen bonding likely contributes to restrict the available conformational space and consequently is of great help for further computations. Potential energy maps for rotation around the two bonds connecting the amide moieties to the central aromatic ring were calculated (Figure S1, Scheme S2). Four different derivatives were studied: 2-hydroxyisophthalic-1,3-dicarboxamide **12**, the corresponding anion **12⁻**, isophthalic acid dicarboxamide **13**, and pyridine-2,6-dicarboxamide **14**. All dihedral <OCCC angles were systematically varied between -180° and 180° in 60 steps of 6° and for each step the rest of the molecule was re-optimized. Two of the species, i.e. **12⁻** and **14** are capable of forming internal hydrogen bonds between the amide NH protons and the central phenolate oxygen or pyridine

nitrogen atom, respectively. For these species, potential energy surfaces are obtained with a local minimum only for the *in/in*-conformation of the two amides (i.e. the two NH groups point towards each other). Neither the *in/out*- nor the *out/out*-conformations are local minima on the potential energy surfaces. Instead, **12** and **13** reveal several local minima for *in/in*-, *in/out*-, and *out/out*-conformations with the *in/out*-arrangement being slightly (by ca. 4 kJ/mol) more favorable. Consequently, these isophthalic acid derivatives have a somewhat higher degree of conformational flexibility and different forms should exist in equilibrium. This has been confirmed in previous studies[6] for macrocycle **5**, which exists in different conformations (Table S3) that are energetically very close to each other.
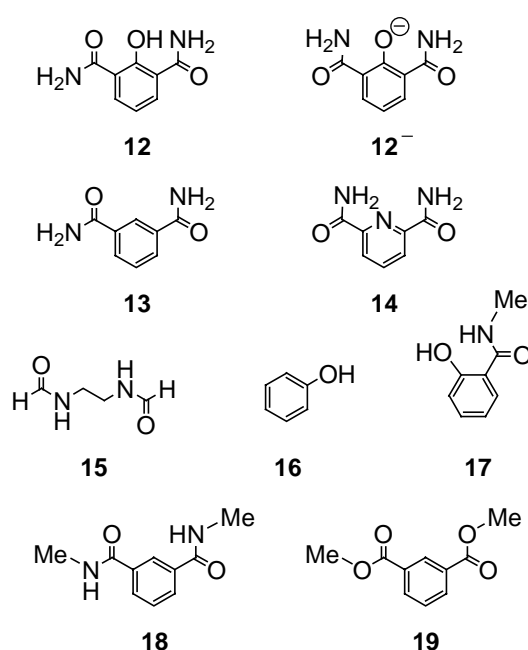
Scheme S2. *Guests for the tetralactam macrocycles used in the calculations to examine conformational properties of building blocks (Figure S1) incorporated in the axle and the wheel and for determining a ranking of binding energies (Table S3).*

Based on this analysis, favorable conformations for axle center piece **10** and its anion **10⁻** were calculated and **10⁻** was combined with the macrocycle **5** to form axle center piece/wheel complexes **10⁻•5**. Indeed, two different conformations are found which are almost equal in energy (Figure S2). The slightly more favorable one represents a non-threaded structure, in which the axle center piece **10⁻** is bound by four hydrogen bonds between its carbonyl groups and the amide groups of the wheel **5**. In this conformation, both amino groups used for stopper attachment point to the same side of the macrocycle and thus, rotaxane formation is prevented when the stoppers are attached to this complex. The second conformation

corresponds to the pseudorotaxane required for the synthesis of the desired rotaxane. Here, the wheel forms two hydrogen bonds to each, the phenolate oxygen atom and one of the carbonyl groups of **10⁻** resulting in a total of four hydrogen bonds between **10⁻** and **5**. Similar structures are found for the complex of **10⁻** with the pyridine wheel **6**. Here, binding of the phenolate in its threaded conformation may occur in two different orientations. The phenolate oxygen may point towards the pyridine nitrogen atom, where on one hand the amide groups are nicely preorganized for hydrogen bonding, but on the other hand the negative charge is closer to the negatively polarized nitrogen atom in the pyridine ring. In the other orientation, the phenolate oxygen points towards the isophthalic dicarboxamide unit. The two conformations are almost the same in energy (Table S3).
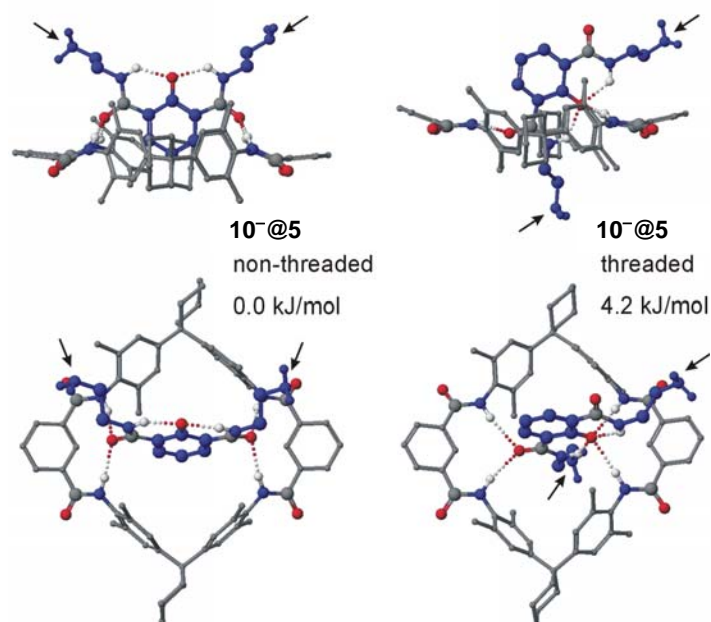
*Figure S2. Non-threaded and threaded axle center piece/wheel complexes **10⁻@5** and their relative AM1 energies. For clarity, hydrogen atoms are omitted. The wheel is shown in grey, the axle center piece in blue. The functional groups involved in hydrogen bonding (dotted lines) are colored according to the CPK model. Black arrows point to the amino groups to which the stoppers are attached.*

With respect to an analysis of the dynamic properties and the switching capability of the rotaxanes through addition of acids and bases, it is important to know at what positions of the axle the wheel may bind most strongly depending on the protonation state of the axle centerpiece. In the next step, AM1 calculations were performed on complexes of wheel **5** with the model compounds **15** - **19** or their corresponding anions (Scheme S2 and Table S3) in

order to identify the most strongly bound sites along the axle. A clear ranking of binding enthalpies is found: A phenol OH group forms only very weak hydrogen bonds with the amide groups of the wheel (ΔH_{assoc} = 14 kJ/mol). Dicarbonyl compounds **15**, **18**, and **19** follow with binding enthalpies of around 50 kJ/mol. Most strongly bound are phenolates **16**⁻ and **17**⁻. The formation of ionic hydrogen bonds results in a binding enthalpy of almost 140 kJ/mol for both. Somewhat surprisingly, the binding strength of **17**⁻ is not larger than that of **16**⁻, although **17**⁻ is capable of forming two more hydrogen bonds with the wheel through the amide carbonyl group. One might speculate that binding of the carbonyl group requires a deviation from the phenolate's most favorable position in the wheel cavity which compensates for the additional binding energy of the two new hydrogen bonds.

References and Notes

[1]   P. Ghosh, O. Mermagen, C. A. Schalley, *Chem. Commun*. **2002**, 2628-2629.

[2]   a) F. Vögtle, S. Meier, R. Hoss, *Angew. Chem.* **1992**, *104*, 1628-1631; *Angew. Chem. Int. Ed.* **1992**, *31*, 1619-1622; b) a) F. Vögtle, S. Meier, R. Hoss, *Angew. Chem.* **1992**, *104*, 1628-1631; *Angew. Chem. Int. Ed.* **1992**, *31*, 1619-1622.

[3]   H. Günther, *NMR-Spektroskopie*, 3rd ed., Thieme, Stuttgart: 1992, p. 314-317.

[4]   G. M. Sheldrick, SHELXL-97, Program for Structure Solutions, University of Göttingen, 1997.

[5]   M. J. S. Dewar, E. G. Zoebisch, E. F. Healy, J. J. P. Stewart, *J. Am. Chem. Soc.* **1985**, *107*, 3902-3209.

[6]   A validation of the AM1 semi-empirical method for the species under study was performed earlier: a) W. Reckien, S. Peyerimhoff, *J. Phys. Chem. A* **2003**, *107*, 9634; b) P. Linnartz, S. Bitter, C. A. Schalley, *Eur. J. Org. Chem.* **2003**, 4819; c) C. A. Schalley, W. Reckien, S. Peyerimhoff, B. Baytekin, F. Vögtle, *Chem. Eur. J.* **2004**, *10*, 4777-4789. In the latter reference, calculations are included which take into account solvent effects.

[7]   CACHE 5.0 for Windows, Fujitsu Ltd. **2001**, Krakow, Poland.

[8]   a) S. J. Weiner, P. A. Kollman, D. A. Case, U. C. Singh, G. Alagona, S. Profeta, P. Weiner, *J. Am. Chem. Soc.* **1984**, *106*, 765-784; b) S. J. Weiner, P. A. Kollman, N. T. Nguyen, D. A. Case, *J. Comput. Chem.* **1987**, *7*, 230-252; c) D. M. Ferguson, P. A. Kollman, *J. Comput. Chem.* **1991**, *12*, 620-626.

[9]   Schrödinger, Inc. 1500 SW First Avenue, Suite 1180, Portland, OR 97201, USA. Also, see: a) F. Mohamadi, N. G. Richards, W. C. Guida, R. Liskamp, C. Caulfield, G. Chang, T. Hendrickson, W. C. Still, *J. Comput. Chem.* **1990**, *11*, 440; b) D. Q. McDonald, W. C. Still, *Tetrahedron Lett.* **1992**, *33*, 7743-7746.